KSÜ Mühendislik Bilimleri Dergisi, 28(2), 2025
Araştırma Makalesi

KSU J Eng Sci, 28(2), 2025
Research Article

Kahramanmaras Sutcu Imam University
Journal of Engineering Sciences

Geliş Tarihi : 09.03.2025
Kabul Tarihi :15.04.2025

Received Date : 09.03.2025
Accepted Date : 15.04.2025

NUMERICAL INVESTIGATION OF THERMAL AND STRUCTURAL BEHAVIOR IN INJECTION-MOLDED FEMUR IMPLANTS

ENJEKSİYON KALIPLAMA İLE ÜRETİLEN FEMUR İMPLANTLARININ ISIL VE YAPISAL DAVRANIŞLARININ SAYISAL OLARAK İNCELENMESİ

Fuat TAN [1*] (ORCID: 0000-0002-4194-5591)
Ahmet Kerem ALKAN [1] (ORCID: 0009-0004-6595-3969)

[1]Balıkesir University, Department of Mechanical Engineering, Balıkesir, Türkiye

*Sorumlu Yazar / Corresponding Author: Fuat TAN, fuattan@balikesir.edu.tr

ABSTRACT

The biomedical applications utilized in this research adopt biocompatible engineering polymers instead of the standard Ti-6Al-4V alloy. The use of Polypropylene (PP), Polyoxymethylene (POM), and Polybutylene Terephthalate (PBT) was explored through the process of injection molding in the manufacture of implants. In examining the various polymers, molding flow, volumetric shrinkage, warpage, and mechanical strength were the parameters that were put under consideration. It was found (using the Autodesk Moldflow Insight software) that the deformation in the Z-axis was the largest for POM with 1.134 mm, followed by PP with 1.102 mm and PBT with 0.987 mm, whereas the volumetric shrinkage rates were computed as 18.05, 18.29, and 16.76, respectively. The Ansys Workbench software simulations demonstrated that a maximum axial force of 45 Nm was applied to the femur-implant model, and the maximum equivalent stress was 112.3 MPa for POM, 89.7 MPa for PP, and 104.2 MPa for PBT. The total deformation values were determined to be 1.24 mm for POM, 1.68 mm for PP, and 1.09 mm for PBT. The key results of this research were that PBT is the ideal material with the utmost dimensional stability and minimal warpage and volumetric shrinkage rates, as well as being the one that is mechanically compatible with the bone. The analyses confirmed that PBT thermoplastic is the more favorable choice among the materials for implant-making using the injection molding technique.

Keywords: Injection molding, implant, femur, FEA, warpage, structural analysis

ÖZET

Bu araştırma, biyomedikal uygulamalarında standart Ti-6Al-4V alaşımı yerine biyouyumlu mühendislik polimerlerini kullanma üzerine yapılmıştır. İmplantların üretimi için enjeksiyon kalıplama prosesinde Polipropilen (PP), Polioksimetilen (POM) ve Polibütilen Tereftalat (PBT) kullanımı incelenmiştir. Kalıp içi akış, hacimsel büzülme, çarpılma ve mekanik dayanım dikkate alınan parametrelerdir. (Autodesk Moldflow Insight yazılımı kullanılarak) Z eksenindeki deformasyon için, en büyük deformasyon 1.134 mm ile POM, ardından 1.102 mm ile PP ve 0.987 mm ile PBT iken hacimsel büzülme oranları sırasıyla 18.05, 18.29 ve 16.76 olarak hesaplanmıştır. Ansys Workbench yazılım simülasyonları, femur implant modeline maksimum 45 Nm eksenel kuvvetin uygulandığını ve maksimum eşdeğer gerilmenin POM için 112,3 MPa, PP için 89,7 MPa ve PBT için 104,2 MPa olduğunu göstermektedir. POM için toplam deformasyon değerinin 1,24 mm, PP için 1,68 mm ve PBT için 1,09 mm olduğu belirlenmiştir. Araştırmada, PBT'nin en yüksek boyutsal stabiliteye ve minimum eğrilme ve hacimsel büzülme oranlarına sahip ideal bir malzeme olduğu ve kemikle mekanik olarak uyumlu bir malzeme olduğu temel sonucuna varılmıştır. Analizler, PBT termoplastik malzemenin, enjeksiyon kalıplama tekniği kullanılarak implant yapımı için daha uygun bir seçim olduğunu göstermektedir.

Anahtar Kelimeler: Enjeksiyon kalıpçılık, implant, femur, FEA, çarpılma, yapısal analiz

ToCite: TAN, F., & ALKAN, A. K., (2025). NUMERICAL INVESTIGATION OF THERMAL AND STRUCTURAL BEHAVIOR IN INJECTION-MOLDED FEMUR IMPLANTS. *Kahramanmaras Sutcu Imam University Journal of Engineering Sciences*, 28(2), 1007-1019.

INTRODUCTION

Injection molding is a widely used manufacturing method that is carried out with process parameters selected according to the characteristic properties of thermoplastics (Fu et al., 2020). In injection molding, which is used in many fields, mold design, product warpage, optimal injection points, and the effects of different materials are important research topics. Computer-aided software ensures the most optimal conditions (Nuruzzaman et al., 2016). The use of polymers and polymer composites in biomaterials and within the human body is quite common. They are used in applications such as hip prostheses, bone cement, tissue engineering, polyethylene-based knee prostheses, dental prostheses, and orthopedic prostheses (Shırdar et al., 2019; Bressan et al., 2011; Bıswal et al., 2020; Gumustas et al., 2018; Saad et al., 2018).

Adam and Lih-Sheng produced porous and interconnected foamed structures using PLA and PVOH with salt particles as molds. These materials have the potential to be used as scaffolds in tissue engineering through injection molding (Adam et al., 2010). Surace et al. manufactured a microfilter for biomedical applications using POM material. To ensure fulfillment during production, they optimized process parameters such as melt temperature, injection speed, mold temperature, holding pressure and time, cooling time, and pressure limit (Surace et al., 2016). Chang and Sophia implanted six alginate implants on sheep using the injection molding process. After six months, the implants were removed and compared with the cartilage in the ear. It was determined that proteoglycan and collagen content reached 80% of the natural tissue value. Hydraulic permeability was measured at 74% and 105% (Chang et al., 2003). Tan et al. used the melt blending method to produce micro bone screws with strength and toughness properties. They shaped these screws using the micro-injection molding process with PLLA and PVDF materials (Tan et al., 2024). Zhao et al. developed an injection-molded PMMA coating for pre-coating metal prostheses. During the injection process, water immersion and splitting methods were used to reduce residual stress to 5 MPa (Zhao et al., 2001).

Gogolewski et al. investigated the tissue response and in vivo molecular stability of injection-molded PLA, PHB, and PHB/VA. The degradation of PHB and PHB/VA polymers was lower (15-43%) than that of polylactides six months after implantation. However, materials with higher valerate content (19%, 22%) exhibited greater degradation (Gogolewski et al., 1993). Mi et al. characterized TPU/LA thermoplastics as scaffolds for tissue engineering using microcellular molding. Their study demonstrated that PLA/TPU artificial scaffolds have potential applications in tissue engineering (Mi et al., 2013). Brady et al. examined the moldability of PEG-based hydrogels in injection molding for tissue engineering applications, showing their suitability for biomedical material production (Brady et al., 2023). Oroslany and Kovacs analyzed the injection molding process of a biodegradable implant used for tendon fixation. They conducted finite element simulations using different injection points to compare the thermal properties of the implant (Oroslany et al., 2010). Premalatha et al. designed and installed a hot-runner injection molding machine for biomedical product manufacturing (Premalatha et al.,2024). Azdast et al. introduced the production of biodegradable and biocompatible PLA/nanofibril composite foams using high-pressure foam injection molding and mold opening methods (Azdast et al., 2022). Heidari et al. simulated the injection molding process for three types of PLA-based bone screws. They optimized the process using Design of Experiments (DOE) and structural analysis results to minimize tensile and bending deformations of the screws (Heidari et al., 2017).

Zamani et al. analyzed PLA-based filters using Autodesk Moldflow software. They examined the rheological and thermal properties of the selected polymers (Zamani et al., 2022). Sammoura et al. manufactured microneedles using micro-injection molding. They characterized injection parameters such as compression force, injection volume, holding pressure, and temperature for mass production (Sammoura et al., 2007). Bastos et al. developed and optimized the production of a dual-chamber syringe. The injection molding process was simulated using Moldflow software to determine its feasibility. Additionally, Abaqus and Fluent were used to simulate the mechanical and flow behavior (Bastos et al., 2022, Canbolat et al., 2018, Turkan et al., 2019). Maden and Tüfekçi proposed an alternative implant design for femur bones to reduce stress effects. Using the ANSYS engineering software, they reduced axial force-induced stress in the bone by 38.7% and lateral force-induced stress by 28.3% (Maden et al., 2022). İsaincu et al. utilized the finite element method to assess the effect of fiber orientation in tensile specimens. Using PA66 GF30, they performed in-mold simulations with Moldflow software and determined the fiber orientation tensor. They emphasized the significance of mapping and mesh size for the ANSYS model, considering the anisotropic behavior of the material (İsaincu et al., 2021). Kulkarni et al. developed a fiber-reinforced micromechanical finite element model. They determined the fiber orientation using Moldflow and conducted structural analyses with ANSYS. The Moldflow-ANSYS model successfully generated the load-displacement curve for an injection-molded composite material (Kulkarni et al., 2012). Mao et al. simulated the injection molding process of an automobile rear outer door

panel. After the injection process, they analyzed the mechanical properties of the model using ANSYS and HyperWorks (Mao et al., 2022). In a study (Tan and Alkan., 2024), the production efficiency and quality parameters of piezoelectric pumps manufactured by microinjection were optimized. In another study, the injection molding process parameters were optimized using RSM and GWO methods, and it was determined that RSM was more effective, with a 39.4% increase in tensile modulus achieved through 60% fiber reinforcement (Tan, 2020).

This study uses three PP, POM, and PBT engineering plastics, which are commonly used as an alternative to the less utilized Ti-6Al-4V alloy, for femur implants through the injection molding process and performing mechanical analysis. The tendencies of flow, shrinkage, and warpage exhibited by the materials were determined through Autodesk Moldflow Insight, while their mechanical performance under axial loads was evaluated using the finite element method in ANSYS. The study of the problem by comparing the structural and thermal properties of these biocompatible thermoplastics is conducted so that, in the end, the best material for implant production could be chosen, which could consider both manufacturability and mechanical stability. The study introduces an innovative integration of the injection molding process with simulations and finite element modeling to assess the adequacy of biocompatible thermoplastics for femoral implant usage. Unlike former works that were concentrated on either manufacturing or mechanical aspects, this research quantitatively relates the parameters caused by the process, such as warpage, shrinkage, and cooling behavior, to the ensuing mechanical performance under physiological loads. The presented methodology serves as a basis for the prediction of material choice and the design application of the polymeric orthopedic implants.

MATERIALS AND METHODS

Through careful scrutiny of the literature, the high-level plastics PP, POM, and PBT, which can be used to replace the Ti-6Al-4V titanium alloy, were identified as implant components. The preference for these thermoplastics was due to their lightweight, lower cost, biocompatibility, and excellent mechanical strength and manufacturing efficiency. These thermoplastics were selected from the material database of Moldflow Ultimate Insight software for the performed analyses. The following are their commercial product codes: FUNCSTER XLR3200 (PP), Hostaform C 9021 G (POM), and Valox 260HPR (PBT). Table 1 shows the thermophysical properties of the above materials.

Table 1. Mechanical Properties of Materials

Features	Unit	PP	POM	PBT
Melt density	g/cm^3	0.94523	1.16	1.0432
Melt temperature	C	255	210	250
Solid density	g/cm^3	1.1591	1.4208	1.2585
Mold Surface temperature	C	45	90	60
Elastic modulus (E1)	MPA	5540.62	2300	2600
Elastic modulus (E2)	MPA	3674.26	2300	2600
Possoin's ratio (v12)	-	0.407	0.39	0.4
Possoin's ratio (v23)	-	0.412	0.39	0.4
Shear modulus	MPA	1303.8	825	929
Maximum shear stress	MPA	0.25	0.45	0.4
Maximum shear rate	$1/s$	100000	40000	50000

PP is a highly sought-after engineering plastic because it is lightweight and chemically resistant. Its low viscosity enables easy mold filling; conversely, the high volumetric shrinkage rate must be managed with care and skill. POM is strong and wear-resistant, two strengths that make it a great orthopedic material. But the risk of parting lines should also be considered during the injection process. PBT, for another reason, does have the nice property of being a precision part of good quality, with a low part volume shrinkage of the overall material. This makes it manufactured for precision applications. Viscosity-shear rate graphs, determining the flow properties of the materials, analyzing the filling behaviors in the capillarity process, and the melt properties of the materials for the inside of the cavity filling are of great importance. Therefore, each of the graphics showing the comparison of all three plastics is given (Fig. 1). At the low shear rates, POM has the highest viscosity, and hence it needs more injection pressure in the flow relative to PBT, which has the lowest viscosity and is thus easy to fill. This case provides an advantage to the part in mass production in terms of mold filling time. Because low viscosity reduces the material's resistance to flow, the melt can fill the mold easily and in a short period (Boronat et al., 2009).

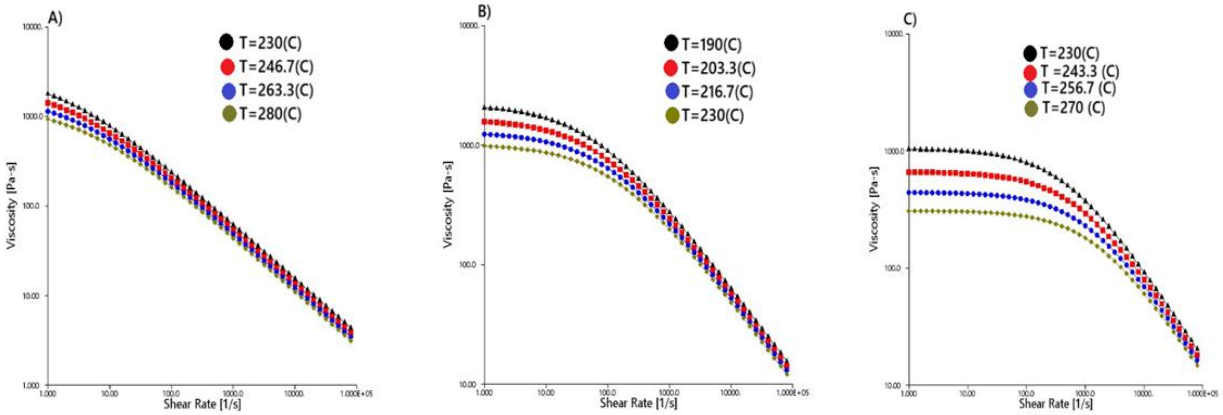

Figure 1. Viscosity vs. Shear Rate of A) PP B) POM C) PBT Materials

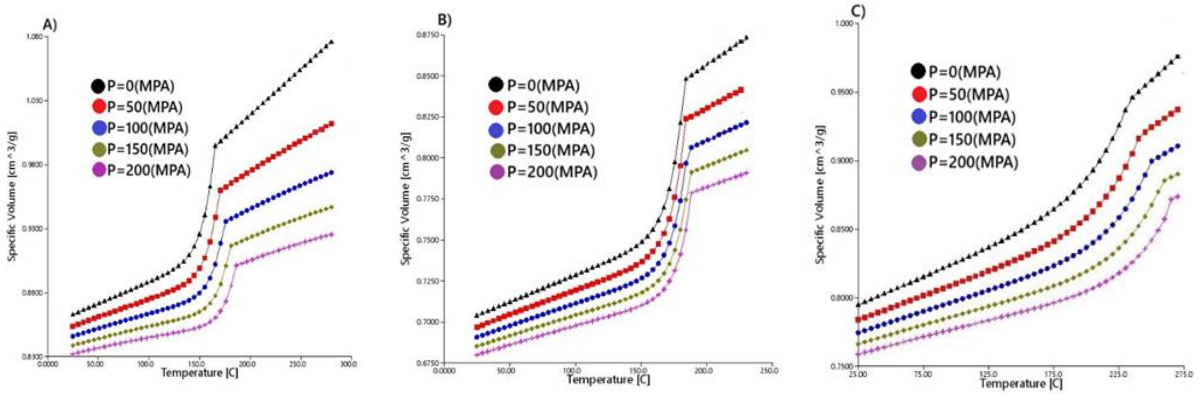

Figure 2. Specific Volume vs. Temperature of A) PP B) POM C) PBT Materials

The following figure comprises the volume-temperature plots of certain materials, which clearly illustrate the dependence of volumetric stability on temperature. These plots are important to know the volumetric shrinkage of the final product (Wang et al., 2020). As depicted in the diagrams, the material's specific volume decreases when the temperature rises while the material is being subjected to high pressure. Consequently, if pressure is kept constant, the temperature increase results in a specific volume increment. PP has the most notable specific volume change with the hotness of the material and is therefore more prone to shrinking under hot conditions, among the materials studied. POM, conversely, is the one that is least influenced by temperature changes, whereas PBT emerges as the material with the lowest thermal expansion because its specific volume is the most stable.

Model

Figure 3 illustrates both the 2D technical drawing and 3D view of the model. The total length of the implant model is 102.27 mm, the wall thickness is 3.45 mm, and the width is 15.86 mm. The model includes six screw holes whose inner diameter is 4.95 mm each.

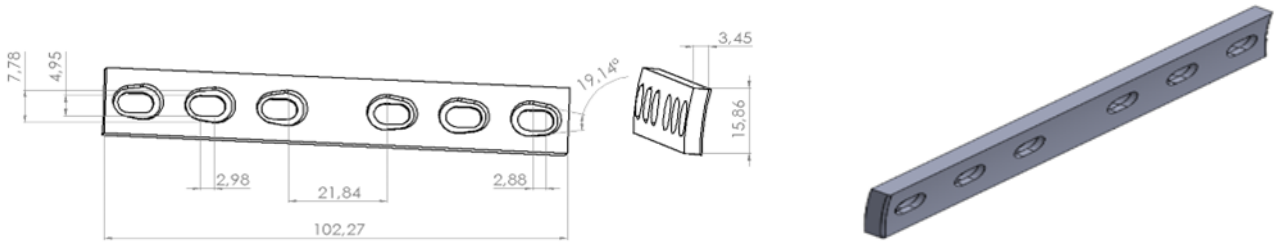

Figure 3. 2D Technical Drawing and 3D View

Mesh

To develop the implant model, the meshing process was used in Moldflow Insight software. The choice of a 3D tetrahedral element type makes it possible to obtain a more accurate representation of the material’s internal volume.

This technique boosts the accuracy of volumetric modeling, and at the same time, it is enriched by a six-layer refinement zone. The mesh structure is mainly 127,489 elements and 24,502 nodes. The aspect ratio, a primary quality measure, was achieved as 2.81 afterward. A mesh model can be viewed in Figure 4.

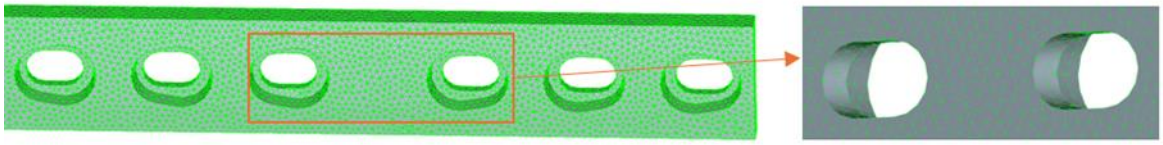

Figure 4. Mesh View

Process Settings

This research tested the simulation of the implant model using the Autodesk Moldflow Insight software filled along with the Fill-Pack-Warpage analysis. The computer-aided manufacturing (CAM) simulation permitted the visualization of POM, PP, and PBT plastic flow in the mold cavity, the cooling rate, the volumetric shrinkage, and the mechanical behavior of the plastics in the process. Based on the result, the CFD analysis was made on a computer with a 12-core AMD64 processor. The fluid behavior was simulated using the Coupled 3D Flow Solver, which ensures a more accurate representation of the viscous behavior of the melt and provides precise injection process simulation. The injection molding machine, which was in the study, is comprised of a spanning injection pressure of the maximum value of 1800 bar and a multiplying force of 70000 kN. Furthermore, the plunger stop intensification ratio was set to 10:1 to maximize the injection conditions.

Fill Analysis

The examination of the fill was the analysis of the injection point's location, the system's flow resistance, and the material's distribution within the mold. The automatic pressure/velocity transition point was found. Material tracking was done through the Level Set method, and flow stability was checked through the Coupled 3D Flow Solver. It was determined that the maximum fill volume and flow rate were the optimum ones to get a uniform mold filling. Concurrently, the filling stage was going on; the maximum fill volume was 4% at each time step. 50 iterations maximum are applied to each step. As the max filling pressure was decided at 4.89 MPa, the computation of total filling time was made in the amount of 1.87 seconds. The maximum speed of the injection machine was assessed in the direction of 5000 cm^3/s. The expressions of the melt temperatures were determined to be 210°C for POM, 255°C for PP, and 250°C for PBT. The mold temperatures were established at 90°C for POM, 45°C for PP, and 60°C for PBT.

The coefficients of heat transfer were established in the following order: 5000 W/m^2K at the filling stage, 2500 W/m^2K in the packing stage, and 1250 W/m^2K in the cooling stage. The analysis further allowed for the identification of the point of automatic pressure/velocity transition. The transition was successfully achieved at an injection pressure level of 4.89 MPa at the fresh fill rate of 99.76%. A system of automatic filling control was implemented, and the process of infusion lasted 1.80 seconds. The nominal flow rate was 2.91 cm^3/s, as was determined. The transition of pressure to velocity occurred at a time of 1.87 seconds with the pressure of 4.89 MPa. The cooling time was set for 20 seconds so the mold could be removed from the part, as the part would be safe.

Pack Analysis

At the packaging stage, the injection pressure was based on the fill pressure-time curve approach. Initially, 80% of the injection pressure was used to fill the mold in 10 seconds and kept at a constant level throughout the process. The total time taken to complete the filler or packing cycle was found to be 31.87 sec. The calculations of the average volumetric shrinkage were done, and the result was that 9.47% is the average volumetric shrinkage of all materials. POM had more volumetric shrinkage than PBT and PP, since the results for the two are 18.05% and 18.29%, respectively. The minimum shrinkage was observed in the case of PBT, with a shrinkage value of 16.76%.

Warpage Analysis

Analysis of the warpage showed that the Z-axis was the most altered. A two-layer aggregation approach was used to obtain a second-order tetrahedron mesh. The analysis method used was an AMG matrix (Automatic Multigrid Solver).

RESULTS

The use of polymers such as POM, PP, and PBT in the injection molding process and their flow behavior, mechanical stability, and production efficiency were the main features of this research. Gate location, warpage, volumetric shrinkage, fill time, cooling time, and clamp force analyses were made considering the in-mold behavior of each material. The study also focused on examining the viscosity, thermal conductivity, and mechanical properties of the mold to determine the flow and solidification process. It was noticed that those flow paths, melt temperatures, and mold temperatures of the materials were likely maximized after the injection parameter optimization, and the processes mentioned above were scrutinized for filling and shrinkage.

Gate Location

The optimization of gate location is essential to the injection molding operations and product fabrication for the regular entrance of the cavity with the filling of it and the minimization of the flow defects. The areas with low flow resistance were considered ideal for the achievement of homogeneous and complete filling. Flow Resistance Indicator and Gating Suitability Simulations, therefore, were the main tools used for the determination of the appropriate positions of the gates. Gate location analysis recognized the gate diameter, flow time, and pressure distribution, with the materials' flow characteristics and viscosity differences as the most relevant ones. The figures of the simulations showed that even though a 2.3 mm gate diameter was used in the POM case to balance flow resistance, there was still some flow resistance encountered. However, a 2.1 mm off-center gate with respect to the midpoint of a PP point accelerator arbor was used for faster filling out the molten resin. Meanwhile, a 2.4 mm gate diameter was also employed for the PBT droplet molding as a measure to suppress the effects of the shrinkage.

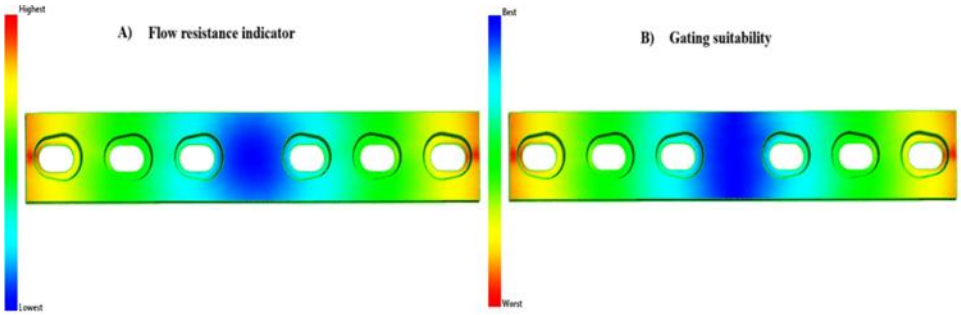

Figure 5. A) Flow Resistance Indicator B) Gating Suitability

Volumetric Shrinkage

Volumetric shrinkage can be described as the volume change that takes place when the melted polymer cools down and hardens within the mold during the injection molding process. The analysis proved that POM and PP reveal major reductions in dimensions, while PBT's decrease is less. The highest values of shrinkage were 18.05% for POM, 18.29% for PP, and 16.76% for PBT. The average values of shrinkage were set as 9.47% for POM, 9.47% for PP, and 7.20% for PBT. Higher shrinkage rates of PP and POM cause the need for longer packing times and a more equal pressure profile to be used in the mold for preservation of the dimensional stability.

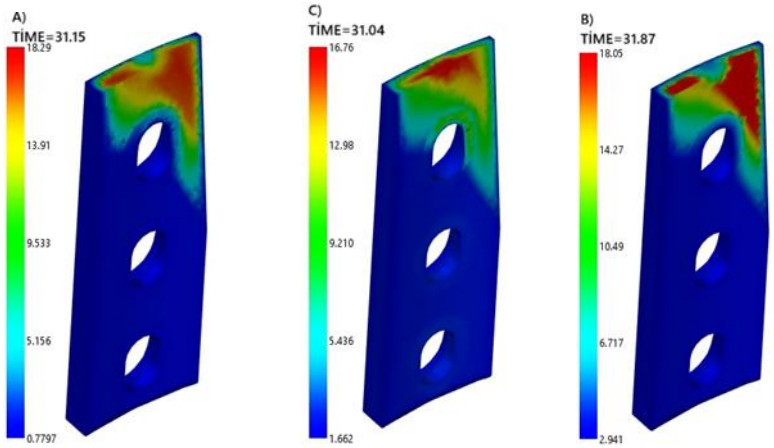

Figure 6. Volumetric Shrinkage: A) PP B) POM C) PBT

In contrast, PBT's lower shrinkage rate results in the fact that a larger part of the deformation is removed after production, and thus, the advantage is dimensional stability. With clamping force being directly proportional to shrinkage, the shrinking factor is also the main player in this case. PBT is the kind of polymer with the minimum level of shrinkage, and hence it assumes the lower clamping force, while POM and PP, with their higher shrinkage will have more stress on the mold. Therefore, the more accurate balancing techniques should be incorporated into the mold design for POM and PP.

Warpage

The warpage analysis was carried out to determine the mechanical stability and dimensional accuracy of the part after the injection molding process. The warpage behavior of POM, PP, and PBT materials was compared, and the maximum displacement values were calculated for different axes.

The identification of the maximum displacement values was made as follows:

- ✓ POM: X: 0.317 mm, Y: 0.252 mm, Z: 1.134 mm
- ✓ PP: X: 0.298 mm, Y: 0.238 mm, Z: 1.102 mm
- ✓ PBT: X: 0.285 mm, Y: 0.221 mm, Z: 0.987 mm

POM was the material causing the alarming warpage, with the maximum Z-axis distance deformation of 1.134 mm, which is a great threat to the dimensional stability of the product. PP had a high level of warpage as well, which was similar to POM. On the other hand, PBT had the smallest warpage values, and it was the most dimensionally stable element.

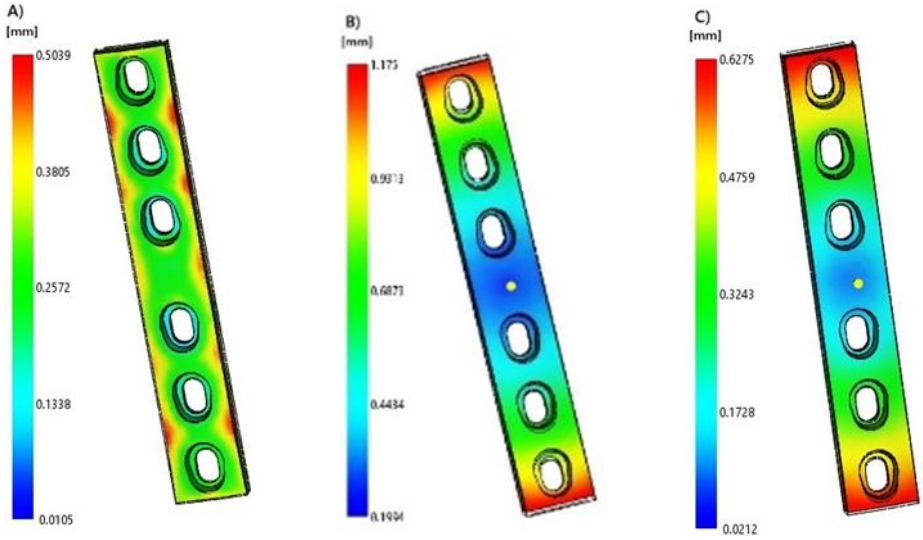

Figure 7. Deflection, All Effects A) PP B) POM C) PBT

Fill Time

The fill-time analysis was conducted to determine the flow rates and filling efficiency of the materials. The simulation revealed flow times of 1.87 s for POM, 1.80 s for PP, and 1.85 s for PBT in the case of filling. PP used to be the least viscous substance, thus using the fastest filling time, whereas POM had the longest fill time because of its high flow resistance. The injection pressures were found to be 4.89 MPa for POM, 4.45 MPa for PP, and 4.73 MPa for PBT. The excessive viscosity of POM has led to the flow resistance increase, which in turn causes a greater pressure requirement. On the contrary, with its low viscosity, PP had the lowest injection pressure needed to finish the filling process more efficiently.

Clamp Force

A study found out the force that is needed to prevent a mold from opening during the injection process. The clamp force is a function of the injection pressure and flow rate. As per the simulated results, the highest clamp values came out to be 0.2063 tons for POM, 0.1529 tons for PP, and 0.2435 tons for PBT. PBT was found to be the mold surface on which the greatest pressure was exerted on which was the reason for it to have the highest clamp force requirement. Nonetheless, POM had a lower clamp force; therefore, uneven pressure distribution was observed because of its high

viscosity. However, PP, unlike its other competitors, required the lowest clamp force since it has low viscosity, which results in smooth flow, and the mold does not experience much stress.

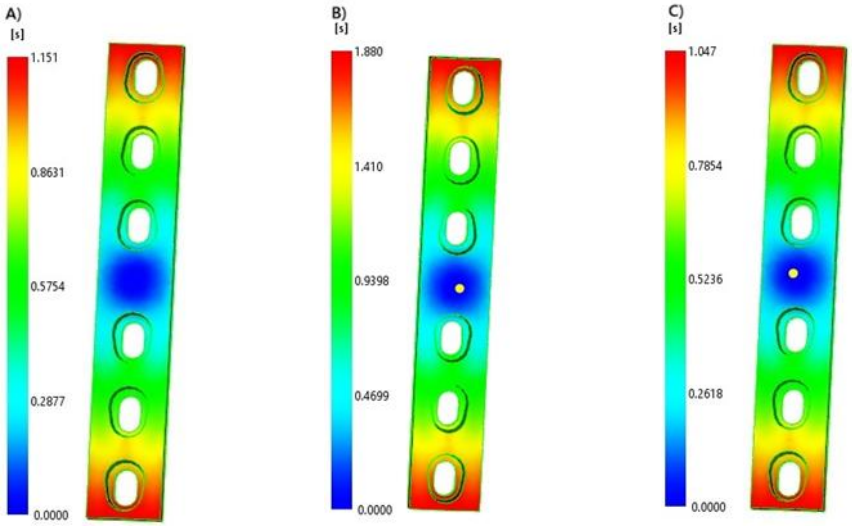

Figure 8. Fill Time Results A) PP B) POM C) PBT

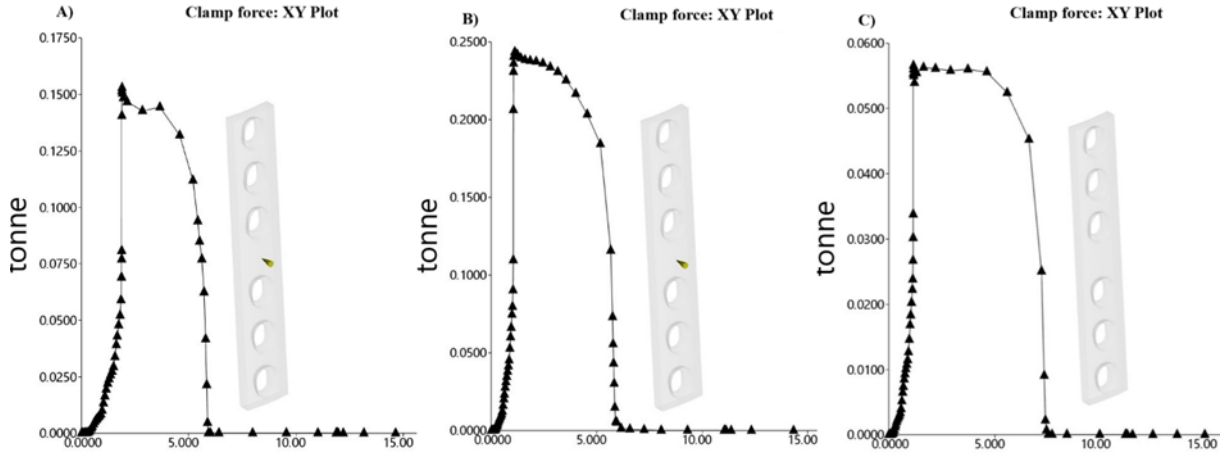

Figure 9. Clamp Force: A) PP B) POM C) PBT

Cooling Time

To investigate and quantify the cooling interval available for the material to get solid inside the mold and then forge stabilization, safely eject it use the situation for cooling-time analysis. The numerical computer simulation results showed that the cooling times totaled 20.3 s, 18.7 s, and 19.5 s (in the case of POM, PP, and PBT, respectively). The reason why PP had the minimum cooling time is that it has the least volume and the highest thermal conductivity. The opposite statement can be made about POM, which means that it needed the most time for cooling, as its crystalline structure is very high. The mold temperatures were stipulated at POM-90°C, PP-45°C, and PBT-60°C. POM's mold, which was set at a higher temperature, thereby the cooling process was protracted, while PP's mold, with a lower temperature, in contrast, allowed a quicker solidifying process. Simultaneously, cooling time is also a major factor that profoundly affects peak volumetric shrinkage and warpage. The outcome of the long-lasting cooling of POM, unlike PP, which had a fast growth of crystals, showed a trend to warpage and a positive effect on the dimensional accuracy, respectively.

STATIC STRUCTURAL ANALYSIS

The study explores the mechanical behavior of the implants made from POM, PP, and PBT, which are produced through the injection molding process using ANSYS Finite Element Analysis (FEA). Simulations were carried out to assess static loads and their effect on bone-implant systems. The strength of the materials was the key parameter

that was used for the assessment of both stress and deformation. To clarify the geometry, the screws were defined as fixed bonds, and the axial load was imposed on the implants to determine the bearing capacity. To ascertain the structural safety of the implants, the distributions of von Mises stress, the maximum value of deformation, and the safety factors were analyzed.

The behavior of the materials under the load was understood through the use of the elastic modulus, the yield strength, and the fracture resistance. The finite element analysis involved the application of an axial torque of 45 Nm for each material according to the stated boundary conditions. The maximum equivalent stress and deformation values were determined. The results of the analysis provided valuable information on the mechanical characteristics of the implants and were helpful in the choice of the most appropriate material for implant design.

Mesh

The horse bone was analyzed. The plate fixation was applied by Ti-6Al-4V screws, and the implants were connected to the femur model. Ansys Workbench was used for the meshing process. The number of nodes in the model was 15,889, and the total number of elements was 29,854; the aspect ratio was 2.81. The boundary inflation with five layers was applied. The mesh density was increased at the location of the implant-bone contact to provide a more even element distribution for better simulation precision.

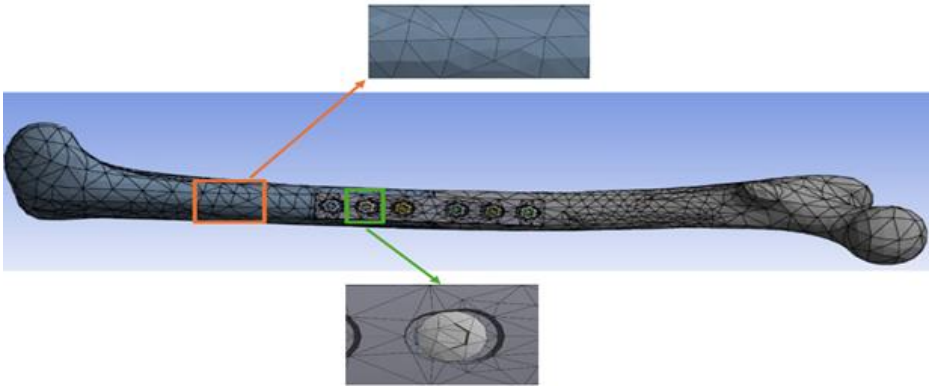

Figure 10. The Meshing Structure of the Femur and Plate Model

Boundary Conditions

Static structural analysis was conducted by considering the implant-femur bone interaction when loading and boundary conditions were defined. The femoral head was stationary, and the applied moment acted on the bone structure. A 15 Nm moment was input to the model. The proximal epiphysis was immobilized, while the distal epiphysis was left free. To elucidate the effect of the moment on the bone-implant system, the load was applied distal from the bone, and the support was located at the femoral head (Maden et al.,2022).

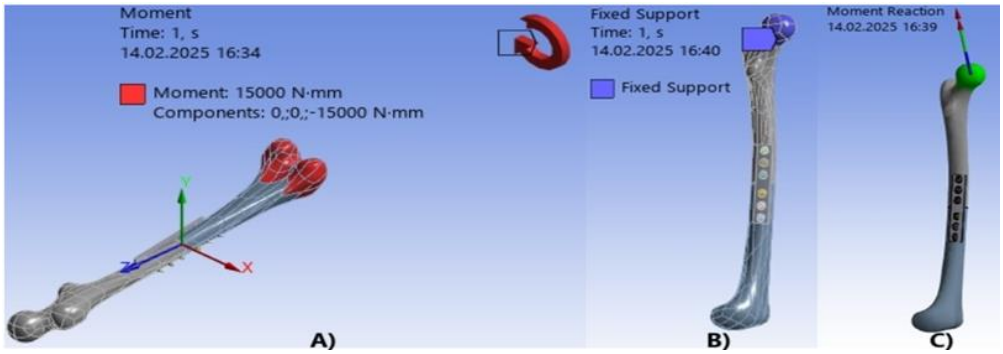

Figure 11. A) Moment B) Fixed Support C) Moment Reaction

By static analysis, the nature of the bending moment will be used instead, and it will be incremented in three stages from 15 Nm to 45 Nm. Each load was assigned a 3-second duration in a linear load increase fashion. "Deformable" type was given to the contact side between bone and implant, and then the pressure distribution in the contact regions was predicted. The friction coefficient between the surface of the implant and the bone was set to 0.3, and the contact conditions were described by using the "Surface to Surface Contact" method. The femur model divided the cortical

and trabecular bone regions. The Young's modulus was given as 17 GPa for the cortical bone and 1 GPa for the trabecular bone. The reason behind this was the accurate emulation of their mechanical properties.

Total Deformation Results

The deformation behavior of POM, PP, and PBT implants under axial load was compared in the simulations conducted in ANSYS. Here, the minimum deformation of the POM implant was 0.099 mm, the maximum was 5.9876 mm, and the average was 0.6358 mm. The minimum deformation of the PP implant was 0.097 mm, the maximum was 5.9449 mm, and the average was 0.6292 mm. The minimum deformation of PBT implant was 0.098 mm, the maximum was 5.9777 mm, and the average was 0.6340 mm. Results show that PP had the lowest average deformation, against which the cases of POM and PBT showed fairly higher values are negligible, although these materials had equal deformation behavior in the case of axial loading.

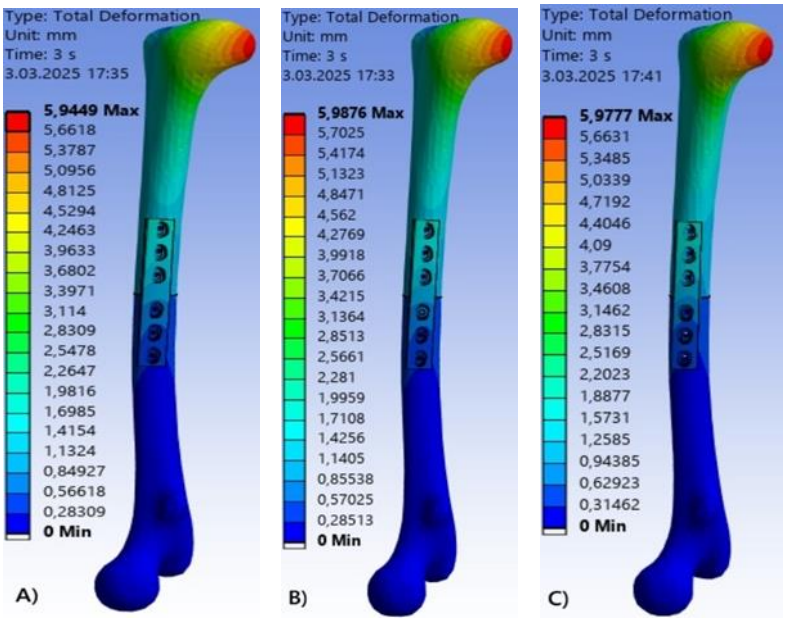

Figure 12. Total Deformation A) PP B) POM C) PBT

The data presents us with the fact that even though all materials have a similar range of deformation, the value of the maximum deformation of the PBT implant is still less than that of the other two materials. According to this evidence, PBT can be seen as a plastic material with high mechanical resistance in loading conditions. Plus, PP had the greatest deformation rates, which means it was the most susceptible to shape changes due to the load. On the other hand, the high strength that comes with POM was not enough to make it more favorable in dimensional stability, as it gave a higher deformation value in comparison with PBT. At the end of this analysis, PBT came off as the best material among the set of options in case the material's mechanical stability is of crucial importance, since it has much lower deformation values. The results suggest that PBT is a highly promising option for injection-molded implants due to its toughness and its good compatibility with bone material.

Equivalent Stress Results

Here, the investigation determined the equivalent (von Mises) stress distributions of POM, PP, and PBT implants. The critical parameters, such as the maximum stress values, such as under load, were analyzed and compared for each material. The examination reports indicate a minimum stress value of 0.00547 MPa for the POM implant and a maximum stress value of 316.36 MPa. The PP implant displayed a minimum stress value of 0.00944 MPa and a maximum stress value of 311.73 MPa. In the case of the PBT implant, the minimum stress value is recorded as 0.00634 MPa, and the maximum stress value is 319.03 MPa. The analysis revealed that the highest stress values were found around the interfacing areas of the implant. Major stresses were most likely found in the areas with the screws at. These data reveal that the screw areas are crucial to the implantation's structural integrity, as they are under heavy loads when in use.

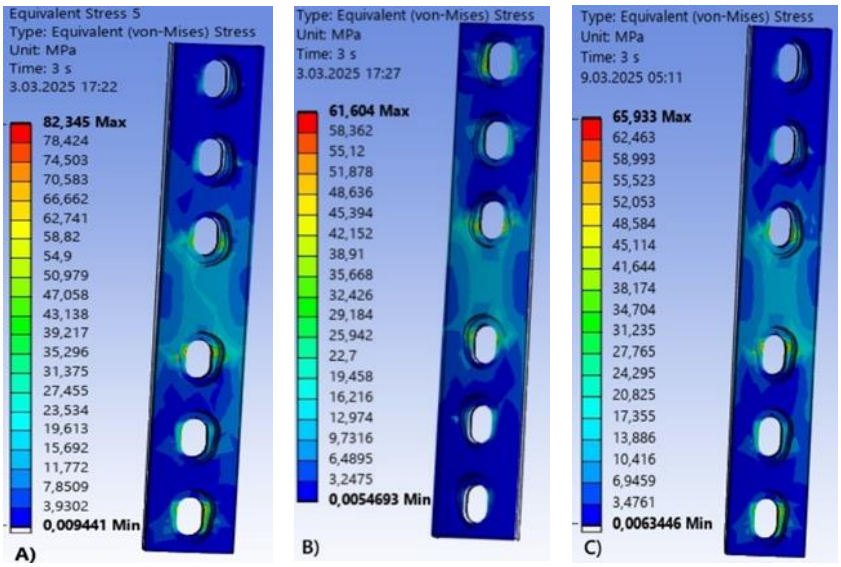

Figure 13. Equivalent Stress A) PP B) POM C) PBT

Global evaluation of the implant appeared to be the best in terms of the maximum stress among all three material options. However, the implementation of the average stress for all the materials showed identical outcomes. Regardless of this, it was noticed that the maximum stress values of POM and PP were lower in comparison to those of PBT. However, in terms of deformation, PBT presented the highest structural stability. In this line, the result showed that PBT was the most cost-effective material for stability and osseoproduction under various loads. However, POM may be more suitable in certain applications if its high resistance is needed based on the implant's design and mechanical specifications.

CONCLUSIONS

This article deals with the study that focused on the structural and thermal characteristics of the femur implants made from the injected molded POM, PP, and PBT. The Moldflow simulations exhibited that PBT had the least warpage (0.987 mm separate to the Z-axis) and volumetric shrinkage (16.76%), and therefore, it was considered the most dimensionally stable material. POM underwent the most deformation, with 18.05% volumetric shrinkage and 1.134 of the warpage, which points to the most malleable material as the one with the most shape changes. Comparatively, PP, because of its low viscosity, had the shortest fill time (1.80 s) and the lowest injection pressure (4.45 MPa). However, PP outperformed PBT in that it shrank and deformed more in comparison. The ANSYS structural analysis, on the other hand, offered that PBT had the smallest total deformation under a 45 Nm load (1.09 mm), and POM (1.24 mm) and PP (1.68 mm) exhibited the largest deformations. On the other hand, the equivalent stress analysis demonstrated that the maximum von Mises stress values were approximately the same for all materials (PBT: 319.03 MPa, POM: 316.36 MPa, PP: 311.73 MPa).

To sum up, the reconstructed femur produced by the injection molding method, which has PBT as its material, is a better alternative. Its poor characteristics are low warpage, low shrinkage, and high mechanical strength. Despite its high strength properties, the high shrinkage and warpage rates of POM necessitate careful process optimization during manufacturing. PP, however, was the most deformed part of all the implants exposed to the load. It is used for non-load-bearing implant applications since the modulus of elasticity of the material is very low. Considering the balance between the manufacturing process and mechanical performance, application, and results, PBT is recommended as the most optimal material for injection-molded femur implants.

In addition to these findings, the present study offers a meaningful contribution by proving the efficiency of combining Moldflow with a finite element-based structural analysis to evaluate the injection-molded biomedical implants. This study enables a precise examination of process-dependent deformation and stress behavior by using different thermal and mechanical simulations, also providing a working framework for implant material selection. The fact that PBT was seen as a good alternative to the usual metallic alloys like Ti-6Al-4V is very important since PBT is better concerning dimensional stability and mechanical compatibility under physiological loads. The other aspect of this study, which states the ability of new thermoplastics to be used in biomedical applications, especially when lightweight structure, biocompatibility, and manufacturing efficiency are factors to be considered, is very

strong. These findings could be used as a reference for studies focused on cost-effective and performance-optimized polymer based implants.

REFERENCES

Azdast, T., Shirinbayan, M., & Rezaei, A. (2022). High-pressure foam injection molding of polylactide/nano-fibril composites with mold opening. In *Polymeric Foams* (pp. 129-139). CRC Press.

Bressan, E., Favero, V., Gardin, C., Ferroni, L., Iacobellis, L., Favero, L., ... & Zavan, B. (2011). Biopolymers for hard and soft engineered tissues: application in odontoiatric and plastic surgery field. *Polymers*, *3*(1), 509-526.

Biswal, T., BadJena, S. K., & Pradhan, D. (2020). Synthesis of polymer composite materials and their biomedical applications. *Materials Today: Proceedings*, *30*, 305-315.

Brady, S. R., Nguyen, H. T., Patel, D. K., & Jones, A. M. (2023). Engineering synthetic poly(ethylene) glycol-based hydrogels compatible with injection molding biofabrication. *Journal of Biomedical Materials Research Part A*, *111*(6), 814-824.

Bastos, L., Rodrigues, P., & Almeida, J. (2022). Design and development of a novel double-chamber syringe concept for venous catheterization. *Medical Engineering & Physics*, *100*, 103757.

Boronat, T., Ferrer, J. M., & Sánchez, J. (2009). Influence of temperature and shear rate on the rheology and processability of reprocessed ABS in injection molding process. *Journal of Materials Processing Technology*, *209*(5), 2735-2745.

Chang, S. C. N., Hansbrough, J. F., Wheeler, E. S., & Wong, V. W. (2003). Tissue engineering of autologous cartilage for craniofacial reconstruction by injection molding. *Plastic and Reconstructive Surgery*, *112*(3), 793-799.

Canbolat A.S., Bademlioglu A.H. & Kaynakli Ö. (2022). Thermohydraulic performance optimization of automobile radiators using statistical approaches. *Journal of Thermal Science and Engineering Applications*, *14(5)*, 051014.

Fu, H., Xu, H., Liu, Y., Yang, Z., Kormakov, S., Wu, D., & Sun, J. (2020). Overview of injection molding technology for processing polymers and their composites. *ES Materials & Manufacturing*, *8*(20), 3-23.

Gumustas, B., & Sismanoglu, S. (2018). Effectiveness of different resin composite materials for repairing noncarious amalgam margin defects. *Journal of Conservative Dentistry and Endodontics*, *21*(6), 627-631.

Gogolewskı, S., Jovanovic, M., Perren, S. M., Dillon, J. G., & Hughes, M. K. (1993). Tissue response and in vivo degradation of selected polyhydroxyacids: Polylactides (PLA), poly(3-hydroxybutyrate) (PHB), and poly(3-hydroxybutyrate-co-3-hydroxyvalerate) (PHB/VA). *Journal of Biomedical Materials Research*, *27*(9), 1135-1148.

Heıdarı, B. S., Rezvani, S., & Ghanbari, S. (2017). Simulation of mechanical behavior and optimization of simulated injection molding process for PLA-based antibacterial composite and nanocomposite bone screws using central composite design. *Journal of the Mechanical Behavior of Biomedical Materials*, *65*, 160-176.

Isaıncu, A., Yazdanbakhsh, A. H., & Sharifi, H. H. (2021). Numerical investigation on the influence of fiber orientation mapping procedure to the mechanical response of short-fiber reinforced composites using Moldflow, Digimat, and Ansys software. *Materials Today: Proceedings*, *45*, 4304-4309.

Kramschuster, A., & Turng, L.-S. (2010). An injection molding process for manufacturing highly porous and interconnected biodegradable polymer matrices for use as tissue engineering scaffolds. *Journal of Biomedical Materials Research Part B: Applied Biomaterials*, *92*(2), 366-376.

Kulkarnı, A., Patel, R., & Singh, B. (2012). Modeling of short fiber reinforced injection moulded composite. In *IOP Conference Series: Materials Science and Engineering* (p. 012025). IOP Publishing.

Lee, C. S., Kim, S. H., Park, J. H., & Lee, J. H. (2019). Investigation on very high cycle fatigue of PA66-GF30 GFRP based on fiber orientation. *Composites Science and Technology*, *180*, 94-100.

Maden, O., & Tüfekçi, K. (2022). İnsan femurunda eksenel ve yanal darbe yüküne maruz kalan kemik-implant sisteminin analizi. *Düzce Üniversitesi Bilim ve Teknoloji Dergisi, 12*(1), 112-120.

Mao, H., Wang, Y., & Yang, D. (2022). Otomotiv arka kapı panelinin enjeksiyon kalıplama prosesi simülasyonu ve kalıp tasarımı çalışması. *Mekanik Bilim ve Teknoloji Dergisi*, *36*(5), 2331-2344.

Mi, H.-Y., Jing, X., Liu, Y., & Li, Z. (2013). Characterization of thermoplastic polyurethane/polylactic acid (TPU/PLA) tissue engineering scaffolds fabricated by microcellular injection molding. *Materials Science and Engineering: C, 33*(8), 4767-4776.

Nuruzzaman, D. M., Kusaseh, N., Basri, S., Oumer, A. N., & Hamedon, Z. (2016, February). Modeling and flow analysis of pure nylon polymer for injection molding process. In *IOP Conference Series: Materials Science and Engineering* (Vol. 114, No. 1, p. 012043). IOP Publishing.

Oroszlány, Á., & Kovács, J. G. (2010). Gate type influence on thermal characteristics of injection molded biodegradable interference screws for ACL reconstruction. *International Communications in Heat and Mass Transfer, 37*(7), 766-769.

Premalatha, S., Kumar, R., & Singh, A. (2024). Injection molding hot runner machine. In *2024 International Conference on Power, Energy, Control and Transmission Systems (ICPECTS)* (pp. 1-4). IEEE.

Sammoura, F., Ho, C. M., Lin, L., & Pisano, A. P. (2007). Polymeric microneedle fabrication using a microinjection molding technique. *Microsystem Technologies, 13*, 517-522.

Shirdar, M. R., Farajpour, N., Shahbazian-Yassar, R., & Shokuhfar, T. (2019). Nanocomposite materials in orthopedic applications. *Frontiers of Chemical Science and Engineering*, *13*, 1-13.

Saad, M., Akhtar, S., & Srivastava, S. (2018). Composite polymer in orthopedic implants: A review. *Materials Today: Proceedings*, *5*(9), 20224-20231.

Surace, R., Fassi, I., Previtali, B., & Annoni, M. (2016). Design and fabrication of a polymeric microfilter for medical applications. *Journal of Micro-and Nano-Manufacturing*, *4*(1), 011006.

Tan, F. (2020). Experimental investigation of mechanical properties for injection molded pa66+ pa6i/6t composite using rsm and grey wolf optimization. *El-Cezeri*, *7*(2), 835-847.

Tan, J., Zhang, Y., Liu, W., Wang, X., & Zhou, L. (2024). Fabricating high-performance biomedical PLLA/PVDF blend micro bone screws through in situ structuring of oriented PVDF submicron fibers in microinjection molding. *Composites Part B: Engineering, 281*, 111567.

Tan, F., & Alkan, A. K. (2024). Effect of Cooling Parameters on In-Mold Flow Behavior in the Microinjection Molding of Piezoelectric Pumps. *International Journal of Automotive Science And Technology*, *8*(4), 467-475.

Turkan, B., Canbolat, A.S. & Etemoglu, A.B. (2019). Numerical investigation of multiphase transport model for hot-air drying of food. *Journal of Agricultural Sciences, 25(4),* 518-529.

Wang, J., Liu, Y., Zhang, H., & Chen, L. (2020). Measurement of specific volume of polymers under simulated injection molding processes. *Materials & Design, 196*, 109136.

Zhao, W., Zhang, H., Liu, Y., & Wang, J. (2001). Development of PMMA-precoating metal prostheses via injection molding: Residual stresses. *Journal of Biomedical Materials Research, 58*(4), 456-462.

Zamanı, M. H., Yazdanbakhsh, A. H., & Sharifi, H. H. (2022). Investigation of ventilator's polymeric split filter production with injection molding process using Autodesk Moldflow software.